Tokai J Exp Clin Med., Vol. 35, No. 4, pp. 152-164, 2010

Protein Oxidative Damage and Heme Oxygenase in Sunlight-exposed Human Skin: Roles of MAPK Responses to Oxidative Stress

Emiko AKASAKA[*1], Susumu TAKEKOSHI[*2], Yosuke HORIKOSHI[*2], Kentarou TORIUMI[*2], Norihiro IKOMA[*1], Tomotaka MABUCHI[*1], Shiho TAMIYA[*1], Takashi MATSUYAMA[*1] and Akira OZAWA[*1]

[*1]*Department of Dermatology, Tokai University School of Medicine*
[*2]*Department of Pathology, Tokai University School of Medicine*

(Received September 8, 2010; Accepted October 28, 2010)

Oxidative stress derived from ultraviolet (UV) light in sunlight induces different hazardous effects in the skin, including sunburn, photo-aging and DNA mutagenesis. In this study, the protein-bound lipid peroxidation products 4-hydroxy-2-nonenal (HNE) and the oxidative DNA damage marker 8-hydroxy-2' - deoxyguanosine (8OHdG) were investigated in chronically sun-exposed and sun-protected human skins using immunohistochemistry. The levels of antioxidative enzymes, such as heme oxygenase 1 and 2, Cu/Zn-SOD, Mn-SOD and catalase, were also examined. Oxidative stress is also implicated in the activation of signal transduction pathways, such as mitogen-activated protein kinase (MAPK). Therefore, the expression and distribution of phosphorylated p38 MAPK, phosphorylated Jun N-terminal kinase (JNK) and phosphorylated extracellular signal-regulated kinase (ERK) were observed. Skin specimens were obtained from the surgical margins. Chronically sunlight-exposed skin samples were taken from the ante-auricular (n = 10) and sunlight-protected skin samples were taken from the post-auricular (n = 10). HNE was increased in the chronically sunlight-exposed skin but not in the sunlight-protected skin. The expression of heme oxygenase-2 was markedly increased in the sunlight-exposed skin compared with the sun-protected skin. In contrast, the intensity of immunostaining of Cu/Zn-SOD, Mn-SOD and catalase was not different between the two areas. Phosphorylated p38 MAPK and phosphorylated JNK accumulated in the ante-auricular dermis and epidermis, respectively. These data show that particular anti-oxidative enzymes function as protective factors in chronically sunlight-exposed human skin. Taken together, our results suggest (1) antioxidative effects of heme oxygenase-2 in chronically sunlight-exposed human skin, and that (2) activation of p38 MAPK may be responsible for oxidative stress.

Key words: normal human skin, oxidative stress, antioxidative enzyme, mitogen-activated protein kinase.

INTRODUCTION

Substantial evidence exists to support that aging is associated with the consequence of damage by various endogenous reactive oxygen species (ROS) – the free radical theory of ageing originally proposed by Harman [1]. ROS include superoxide ($O_2^{\cdot-}$) and hydrogen peroxide (H_2O_2) that are derived from oxygen molecules. ROS are involved in a variety of different cellular processes ranging from apoptosis and necrosis to cell proliferation and carcinogenesis. The skin is exposed to a variety of environmental pollutants that are oxidants themselves or can catalyze the formation of ROS directly or indirectly. Oxidative damage to the skin, induced by several exogenous and endogenous factors such as ultraviolet (UV) irradiation, transition metal ions, enzymatic and non-enzymatic antioxidant impairment, has recently been recognized as a key factor of intrinsic and photo-induced skin aging and of several skin disorders such as actinic elastosis and cancer.

8-hydroxy-2'-deoxyguanocine (8-OHdG) is one of the major oxidative base lesions in DNA or nucleotides [2] and is induced following UV irradiation by ROS [3]. 8-OHdG induces G–C to T–A transversion during DNA replication, a possible initiator of carcinogenesis [4]. 4-hydroxy-2-nonenal (HNE) is a major and the most toxic aldehyde and can be an indicator of lipid peroxidation and protein damage. HNE is also considered the second toxic messenger of ROS [5]. HNE reacts with proteins, peptides, phospholipids and nucleic acids, and, therefore, it has multiple cytotoxic, mutagenic, genotoxic and signaling effects including the inhibition of protein and DNA synthesis, enzyme inactivation, stimulation of phospholipase C and chemotaxis of neutrophils, modulation of platelet aggregation, as well as modulation of various gene expression [6]. Interestingly, HNE is associated with elastosis of human skin [7]. However interaction of HNE with extracellular matrix proteins, such as elastin and collagens, remains unclear.

The antioxidative system, including antioxidative enzymes, radical scavengers and chain breakers, limits cell injury induced by ROS. The epidermis of the skin contains a complex enzymatic antioxidant defense system [8]. This system includes enzymes that act directly to detoxify ROS such as superoxide dismutase (SOD) and catalase (CAT), as well as ROS scavengers such

Emiko AKASAKA, Department of Dermatology, Tokai University School of Medicine, 143 Shimokasuya, Isehara, Kanagawa 259-1193, Japan
Tel: +81-463-93-1121 Fax: +81-463-91-1370 E-mail: emiko-a@is.icc.u-tokai.ac.jp

as heme oxygenase [9]. Up regulation of the heme oxygenase (HO) system removes pro-oxidant heme, and thus is cytoprotective. Additionally, the products of the HO pathway including, carbon monoxide, bilirubin, and biliverdin, scavenge reactive oxygen species, thereby inhibit lipid peroxidation [10]. So far three isoforms of HO have been described: HO-2 and HO-3 are constitutively expressed, whereas HO-1 is inducible and is actually identical to the heat shock protein 32 [11].

The MAPK cascades are a group of important pathways in various cellular responses [12]. Three main MAPK have been well characterized: the c-Jun N-terminal kinase (JNK), the p38 mitogen-activated protein kinase (p38 MAPK) and the extracellular signal-regulated protein kinase 1/2 (ERK1/2). ERK can be activated in response to growth factors, oxidative stress [13], and increased intracellular calcium levels or glutamate receptor stimulation. p38 and JNK are activated by oxidative stress such as inflammatory, heat shock, UV and ischemia. Phosphorylation of p38 ensues activation of MAPK-activated protein 2 and transcription factor (ATF) 2, and phosphorylated JNK can activate c-Jun directly [14].

From the point of view of skin oxidative stress, the balance of oxidative stress and the antioxidative system and cellular responses to solar UV-irradiation are of particular importance. In the present study, in order to explore the effects of sunlight-exposure on the protein oxidative damage, antioxidative enzyme expression and corresponding cell signal transduction were examined in the ante-auricular skin (sun-exposed area) and post-auricular skin (sun-protected area).

MATERIALS AND METHODS

Patients and skin samples

Normal skin specimens were obtained from the surgical margins of biopsies taken from both the ante-auricular skin and the post-auricular skin of the same subject. The Tokai University Hospital ethical committee gave approval to the study, and written informed consent was obtained from all individuals. Sun-exposed skin samples were taken from the ante-auricular (n = 10) and sun-protected skin samples were taken from the post-auricular (n = 10). The donors were three male and seven female. The age range was 68–96 years.

Immunohistochemical evaluation of HNE, anti-oxidative enzymes, and MAPK

Human skin specimens were fixed in 10% buffered formalin, dehydrated through successively more concentrated ethanol solutions and finally embedded in paraffin. Tissue sections of 4-μm thickness were prepared for hematoxylin and eosin (H & E) staining and immunohistochemistry (IHC). For IHC, the specimens were dewaxed and rehydrated before staining. Endogenous peroxidase was inactivated with methanol containing 0.3% hydrogen peroxidase (H_2O_2) for 30 min at room temperature. For the immunostaining of HNE, 8-OHdG, HO-1, p38, JNK and ERK, sections were heated in a microwave oven for 5 min in 10 mmol/L citrate buffer (pH6.0). For HO-2, sections were autoclaved at 121˚C in 10 mmol/L citrate buffer (pH6.0) for 10 minutes. For phospho-p38, phospho-JNK and phospho-ERK, sections were autoclaved at 121˚C in 1 mmol/L EDTA2Na (pH7.0) for 10 minutes. For elastin and collagen type I, sections were treated with 0.1% trypsin at 37C˚ for 30 min. Anti-HNE monoclonal antibody (JaICA, Shizuoka, Japan) was used at a 1:10 dilution. Anti-8-OHdG monoclonal antibody (N45.1; JaICA, Hukuroi, Shizuoka, Japan) was tested on sections from nonalcoholic hepatitis for its reactivity and used at a 1:20 dilution. Anti-elastin monoclonal antibody (Abcam, Cambridge, UK) was used at a 1:50 dilution. Anti-collagen type I monoclonal antibody (Abcam, Cambridge, UK) was used at a 1:800 dilution. Anti-HO-1 monoclonal antibody (Stressgen, Ann Arbor, MI, U. S. A.) was used at a 1:50 dilution. Anti-catalase monoclonal antibody (SIGMA, Saint Louis, U. S. A.) was used at a 1:100 dilution. Anti-phospho-p38 monoclonal antibody (Cell Signaling, Danvers, MA, U. S. A.) was used at a 1:50 dilution. Anti-phospho-JNK monoclonal antibody (Cell Signaling, Danvers, MA, U. S. A.) was used at a 1:50 dilution. Anti-phospho-ERK monoclonal antibody (Cell Signaling, Danvers, MA, U. S. A.) was used at a 1:100 dilution. Anti-HO-2 polyclonal antibody (Stressgen, Ann Arber, MI, U. S. A.) was used at a 1:1500 dilution. Anti-Mn-SOD polyclonal antibody (Stressgen, Ann Arber, MI, U. S. A.) was used at a 1:20 dilution. Anti-Cu/Zn-SOD polyclonal antibody (Stressgen, Ann Arber, MI, U. S. A.) was used at a 1:3000 dilution. Following washing with PBS, the signal was amplified with DAKO ENVISION+Kit (DAKO cytomation, Glostrup, Denmark) according to the manufacture's recommendations. Horse radish peroxidase activity was visualized with 3'3-diaminobenzidine tetrahydrochloride. The sections were lightly counterstained with hematoxylin. Immunohistochemical specificity of all the antibodies was confirmed by non-immune immunoglobulins or normal serum as negative controls. For double immunostaining of HNE and elastin or collagen type I, the sections were incubated with anti-elastin monoclonal antibody (Abcam, Cambridge, U. K.) or anti-collagen type I monoclonal antibody (Abcam). After overnight at 4˚C, the signal was amplified with DAKO ENVISION+Kit (DAKO cytomation, Glostrup, Denmark) according to the manufacture's recommendations. Immunoreactivity was visualized by incubation with 3'3-diaminobenzidine tetrahydrochloride. After thorough washing with PBS, the sections were subsequently incubated with anti-HNE monoclonal antibody (JaICA, Shizuoka, Japan) at 4˚C overnight. After washing with PBS, the signals were amplified Avidin-Biotin Complex System (VECTOR LABORATORIES, INC, U. S. A.) according to the manufacture's recommendations followed by visualization with 5-bromo-4-chloro-3-indolyl phosphate and nitroblue tetrazolium chloride (DAKO cytomation, Glostrup, Denmark). For double immunofluorescence staining, frozen human skin tissues were cut into 5 μm sections. These sections were fixed with 2% paraformaldehyde, permeabilized with 0.5% Trition X-100 in PBS and stained after blocking with 10% calf serum in PBS. The primary anti-HNE antibody (JaICA) was used overnight at 4 ˚C. The secondary Alexa Fluor488-conjugated goat antibody against mouse IgG (Invitrogen) was used

for 2 hours at room temperature. And then, Alexa Flour594-labeled mouse anti-collagen type I monoclonal antibody and anti-elastin monoclonal antibody were incubated for 2 hours at room temperature. These antibodies were labeled with Zenon mouse IgG labeling kits (Invitrogen). Imaging of specimens was performed using a LSM-510 META confocal laser scanning microscope (Carl Zeiss MicroImaging, Jena, Germany) and, the META system was employed for computer-assisted image spectrum analysis (Carl Zeiss MicroImaging, Jena, Germany).

Absorption test

Absorption tests were performed with normal human skin to confirm the specificity of the commercial HO-2 antibody (Stressgen). The HO-2 antibody (0.6 μg/ml) was incubated with a blocking peptide (Stressgen; a final concentration of 0, 0.006, 0.066, 0.66, 6.6, or 66.0 μg/ml) at 4˚C overnight; and the immune complex was pelleted by centrifugation, and the supernatant was passed through a 0.45-μm filter before incubation with normal human skin.

Laser microdissection and real-time reverse transcription polymerase chain reaction (RT-PCR)

Tissue sections (6-μm thick) were prepared from the same formalin-fixed paraffin-embedded tissue blocks and counterstained with toluidine blue. For the separation of epidermis and dermis in the ante-auricular skin and the post-auricular skin, a laser microdissection assay was performed using a Laser Microdissection System (LM) (Carl Zeiss MicroImaging, Jena, Germany) coupled with real-time reverse transcriptase PCR. Total RNA was extracted from dissected epidermis or dermis skin sections using TRizol reagent (Invitrogen Life Technologies, Carlsbad, CA, U. S. A.). For synthesis of first-strand cDNA, RNA was reverse transcribed by incubation with random primers and a first-strand cDNA synthesis kit (High Capacity RT kit). Real-time RT-PCR was performed using TaqMan Universal PCR Master Mix (Roche, Branchburg City, NJ, U. S. A.) according to the instructions of the manufacturer, and the specific primers used had the following sequence: human HO-2 primers, 5´- CCT GTA CAC GAT GGG AAA GGA-3´ and 5´- TCC AGG GCA CCT TTG TCT TGT TCA -3´; and human β-actin primers, TaqMan Geneexpression Assay actinß, HS99999903_ml. These primer sets were designed to span one intron to allow identification of genomic contamination. The reaction protocol consisted of the following cycles: 95C˚ for 15 min, 95C˚ for 15 sec and 60C˚ for 1 min for 50 cycles of PCR amplification on an Opticon 2 System (Hercules, CA, U. S. A.). All data were analyzed on an Option monitor 3 (ATTO Corporation, Tokyo)

Statistical analysis

Values are expressed as the mean ± SE. Data from RT-PCR assay were compared by using a paired *t* test. In all cases, $P < 0.05$ was considered significant.

RESULTS

Histopathological analysis

Histopathologial analysis revealed that marked solar elastosis occurred in the ante-auricular dermis compared to the post-auricular dermis (Fig. 1A and 1B). Immunohistochemical study also demonstrated that elastin molecules accumulated in the upper dermis with the exception of the grenz zone (Fig. 1C). Collagen type I was mainly localized in the grenz zone (Fig. 1D).

Production of 8-OHdG and HNE

8-OHdG is a marker of oxidative damage to DNA or nucleotides. Immunoreactivity of 8-OHdG was not detected in either the ante-auricular or post-auricular skins (Fig. 2A and 2B, Table 1). To determine the effect of sunlight exposure on lipid peroxidation, the formation of HNE protein adducts, a marker for lipid peroxidation and index of oxidative stress, was examined by immunohistochemistry. The ante-auricular skins showed strong HNE immunoreactivity in both the epidermis and dermis compared with the post-auricular skins (Fig. 2C and 2D, Table 1). Double immunostaining colocalized HNE and elastin in the ante-auricular dermis but not in the post-auricular dermis (Fig. 3A and 3B). The double immunostaining results are summarized in Table 2. Detailed double immunofluorescence staining analyses of elastin, collagen type I and HNE were carried out and showed that elastin, but not collagen type I, accumulated in HNE-positive extracellular matrix areas of the ante-auricular dermis. Careful inspections of serial sections of these dermis samples revealed that collagen type I did not accumulate in HNE-positive areas (Fig. 4).

Anti-oxidative enzymes

HO-1 is a redox-sensitive inducible protein that provides efficient cytoprotection against oxidative stress, whereas HO-2 is a constitutive isoform of heme oxygenase. Immunohistochemical study demonstrated that HO-1 protein was expressed in both the ante-auricular and post-auricular skins (Fig. 5A and 5B, Table 1). In the epidermis, HO-2 was detected in the cytoplasm both in the ante-auricular and post-auricular skins. In contrast, in the dermis, HO-2 markedly increased in the ante-auricular skins than in the post-auricular skins (Fig. 5C and 5D, Table 1). We next examined the gene expression of HO-2 in formalin-fixed, paraffin-embedded (FFPE) samples of skins using laser microdissection and real-time RT-PCR method. Quantitative mRNA analysis showed significantly increased expression of HO-2 in the ante-auricular dermis as compared to the post-auricular dermis (Fig. 6A, Table 1). Furthermore, the specificity of HO-2 was confirmed by absorption test using a normal human skin. Immunoreactivity was considerably decreased by the absorption. (Fig. 6B, Table 1). Both Mn-SOD and Cu/Zn-SOD were expressed in the accessory structures in the dermis of the post-auricular samples. Mn-SOD was expressed in the granular-like structures around fibroblasts and appendix. Cu/Zn-SOD was stained in the post-auricular and abdominal specimens in the epidermis and appendix. Catalase was expressed in the cytoplasm in the granular-like structure structures in the stratum granulosum epidermis and the nuclei of sebaceous glands in the dermis. No difference was found between the ante-auricular and post-auricular

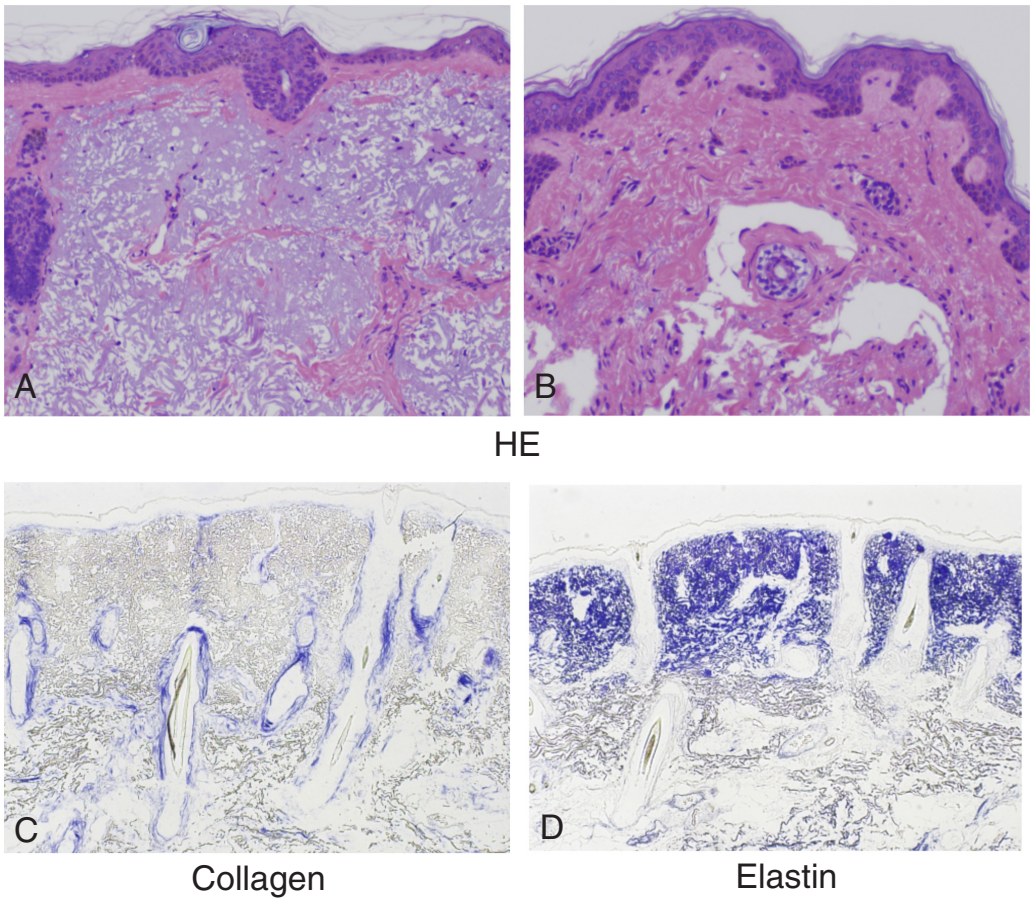

Fig. 1 Histopathological findings in the ante-auricular and post auricular skins. Tissue sections were stained by H & E or immunohistochemistry for elastin and collagen type I. H & E staining (A, B). Immunostaining of elastin (C) and collagen type I (D). Representative sections of the ante-auricular skin (A, C, D) and post-auricular skin (B). (Original magnification x100).

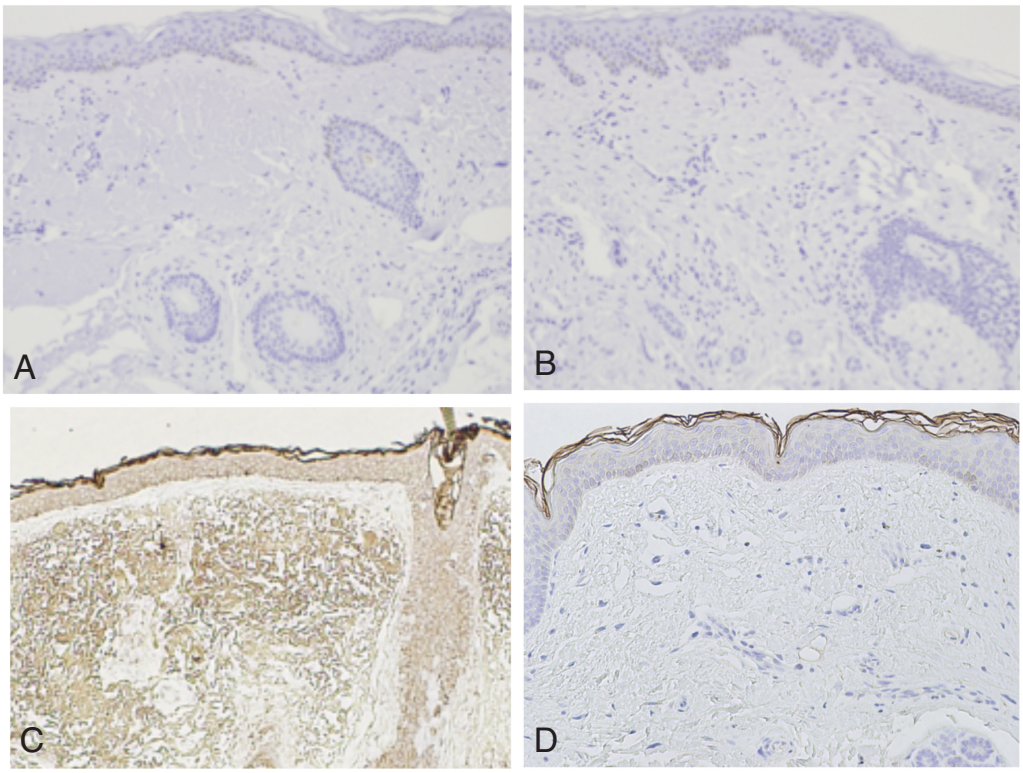

Fig. 2 Immunohistochemistry of the ante-auricular and post-auricular skins with anti-8OHdG antibody and anti-HNE antibody. Staining of 8-OHdG (A, B) and HNE (C, D). Representative sections of the ante-auricular skin (A, C) and post-auricular skin (B, D). (Original magnification x100).

Table 1 8-OHdG, HNE, anti-oxidative enzymes and phosphorylated p38 MAPK, JNK and ERK in the ante- and post-auricular epidermis and dermis.

Location	Case No.	Age/Sex	Immunohistochemistry									
			8-OHdG	HNE	HO-1	HO-2	Cu/Zn SOD	Mn SOD	Catalase	phospho p38	phospho JNK	phospho ERK
ante-auricular/epidermis	1	96/F	−	+	+	++	−	±	±	−	−	+
	2	96/F	−	+	+	+	±	±	+	+	+	+
	3	64/M	−	±	++	++	±	+	±	+	+	+
	4	73/F	−	++	+	+	±	+	+	±	+	++
	5	84/M	−	++	±	++	±	±	±	+	+	++
	6	70/F	−	+	±	+	+	±	+	−	±	+
	7	77/F	−	±	+	++	±	±	±	±	±	±
	8	68/M	−	+	±	+	±	+	+	−	±	+
	9	72/F	−	±	+	+	±	−	+	±	−	+
	10	73/F	−	±	±	+	±	±	±	+	±	+
post-auricular/epidermis	1	96/F	−	±	+	+	−	±	±	−	−	++
	2	96/F	−	+	+	+	+	+	±	+	−	±
	3	65/M	−	±	++	+	±	+	++	−	−	+
	4	74/F	−	±	+	+	±	+	+	−	−	+
	5	85/M	−	±	+	+	±	++	±	+	−	++
	6	84/F	−	±	+	+	±	±	+	−	−	±
	7	91/F	−	±	+	+	++	+	±	+	±	++
	8	69/M	−	±	+	±	++	+	++	+	−	++
	9	74/F	−	−	++	+	+	±	±	+	−	±
	10	75/F	−	−	+	+	±	+	±	+	−	++
ante-auricular/dermis	1	96/F	−	+	−	++	−	±	−	−	−	−
	2	96/F	−	+	±	+	−	-	±	+	−	−
	3	65/M	−	±	−	++	−	++	±	+	−	−
	4	74/F	−	+	++	+	−	++	±	+	−	−
	5	85/M	−	++	±	++	−	+	±	+	−	−
	6	84/F	−	+	+	+	−	++	+	−	−	−
	7	91/F	−	+	±	++	−	++	±	+	−	−
	8	69/M	−	+	±	+	−	+	+	+	−	−
	9	72/F	−	±	±	+	−	±	−	−	−	−
	10	73/F	−	±	±	+	−	-	−	±	−	−
post-auricular/dermis	1	96/F	−	±	±	−	−	±	−	−	−	−
	2	96/F	−	+	−	−	−	−	±	+	−	−
	3	65/M	−	−	±	−	−	++	+	−	−	−
	4	74/F	−	−	+	−	−	++	±	−	−	−
	5	85/M	−	±	±	−	−	+	±	−	−	−
	6	84/F	−	±	+	−	−	++	+	−	−	−
	7	91/F	−	±	+	−	−	++	±	−	−	−
	8	69/M	−	±	+	−	±	+	+	−	−	−
	9	72/F	−	−	++	−	±	±	±	−	−	−
	10	73/F	−	−	+	−	−	−	−	−	−	−

Minus indicates negative; ±, less than 10%; +, 10 to 50%; ++, over 50% of cells.

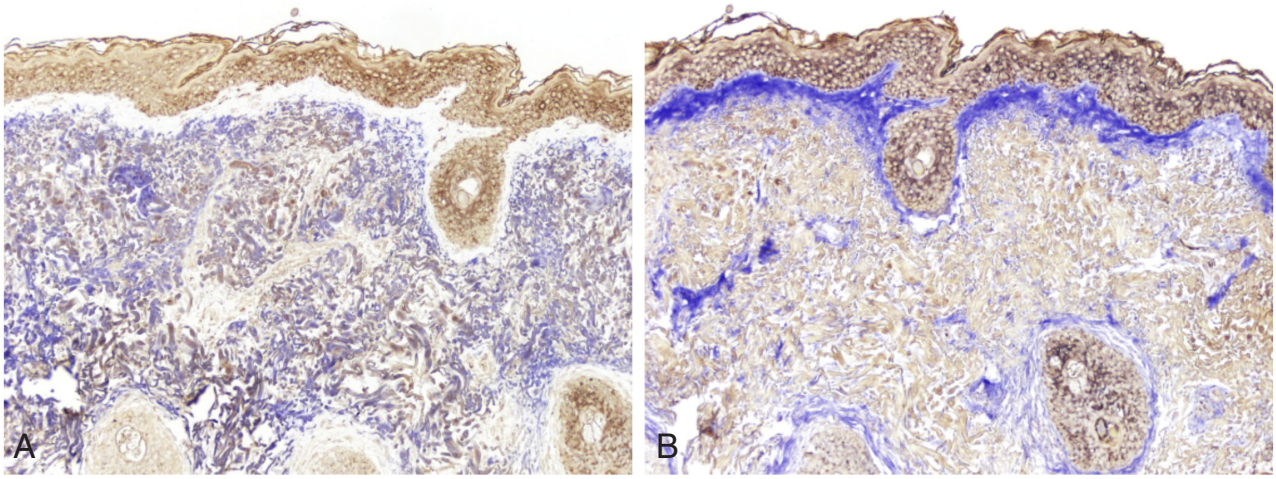

Fig. 3 Colocalization of HNE with elastin and collagen type I in ante-auricular skin. Double immunostaining of HNE and (A) elastin or (B) collage type I was shown. HNE (brown) and elastin or collagen type I (blue). (Original magnification x100).

Table 2 Co-localization of elastin or collagen type I with HNE in the ante-auricular dermis.

Case No.	Age/Sex	HNE	
		elastin	collagen
1	96/F	++	−
2	96/F	++	−
3	64/M	++	−
4	73/F	++	−
5	84/M	++	−
6	70/F	++	−
7	77/F	++	−
8	68/M	++	−
9	72/F	++	−
10	73/F	++	−

Minus indicates negative; ±, less than 10%; +, 10 to 50%; ++, over 50% of double stained-cells.

skins in the intensity of Mn-SOD and Cu/Zn-SOD immunoreactivities (Fig. 7A–F, Table 1).

MAPK signaling

The MAPK pathway is a target of oxidative stress. To determine whether chronic sunlight exposure induces activation of MAPK signaling in human skin, phosphorylation status of p38 MAPK, JNK and ERK was examined following analysis of FFPE specimens by immunohistochemistry using phosphor-specific antibodies (Fig. 8A and 8B, Table 1). Phosphorylated-p38 MAPK (phospho-p38) localized in both ante-auricular and post-auricular epidermis. Phosphorylated-JNK (phospho-JNK) was localized only in the ante-auricular epidermis but not in the post-auricular epidermis or dermis (Fig. 8C and 8D). Phosphorylated ERK (phospho-ERK) was observed the nuclei of inflammatory cells and angio-endothelial cells in skin epidermis (Fig. 8E and 8F). There was no difference in the immunostaining of phospho-ERK between the ante-auricular and post-auricular skins. The immunohistochemistry results are summarized in Table 1.

DISCUSSION

So far, there have been no convincing results to indicate the effect of chronic sunlight exposure on HNE and 8-OHdG levels, the expression of antioxidative enzymes and MAPK signaling in human ante-auricular skin (sunlight exposed area) and post-auricular skin (sunlight protected area). In this study, we demonstrated that chronic sunlight exposure inflicts particular oxidative stress and induces antioxidative enzyme expression and MAPK signaling activation in the human skin without cancer.

The solar ultraviolet radiation spectrum consists of the shorter UVC (200–290 nm), UVB (290–320 nm) and the longer UVA (320–400 nm) radiations. Both UVA and UVB contribute to photocarcinogenesis and photoaging and UVA cannot be regarded to be safer than UVB. The UVB component of sunlight only penetrates into the epidermis while the longer wavelength UVA penetrates deeper into the underlying dermis. We speculate that these differences between UVA and UVB underlie the differences seen in the responses of the epidermis and dermis.

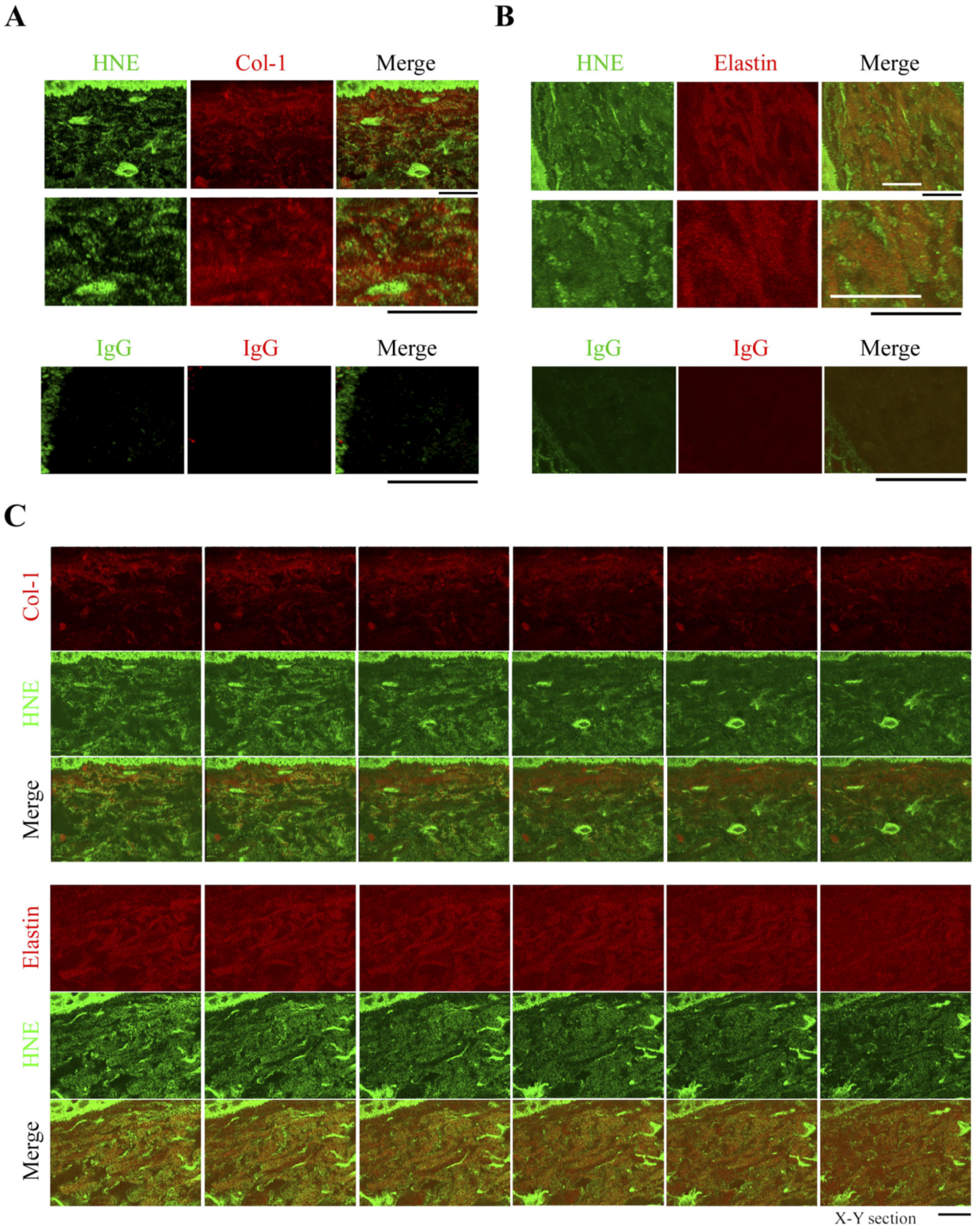

Fig. 4 Double immunofluorescence staining analysis of elastin, collagen type I and HNE. The ante-auricular epidermis stained for collagen type I (red) or elastin (red) with HNE (green). Projected views of confocal sections are presented (A, B). Serial confocal sections of an ante-auricular epidermis stained for collagen type I (red) or elastin (red) and HNE (green) (C). Scale bars: 20 μm.

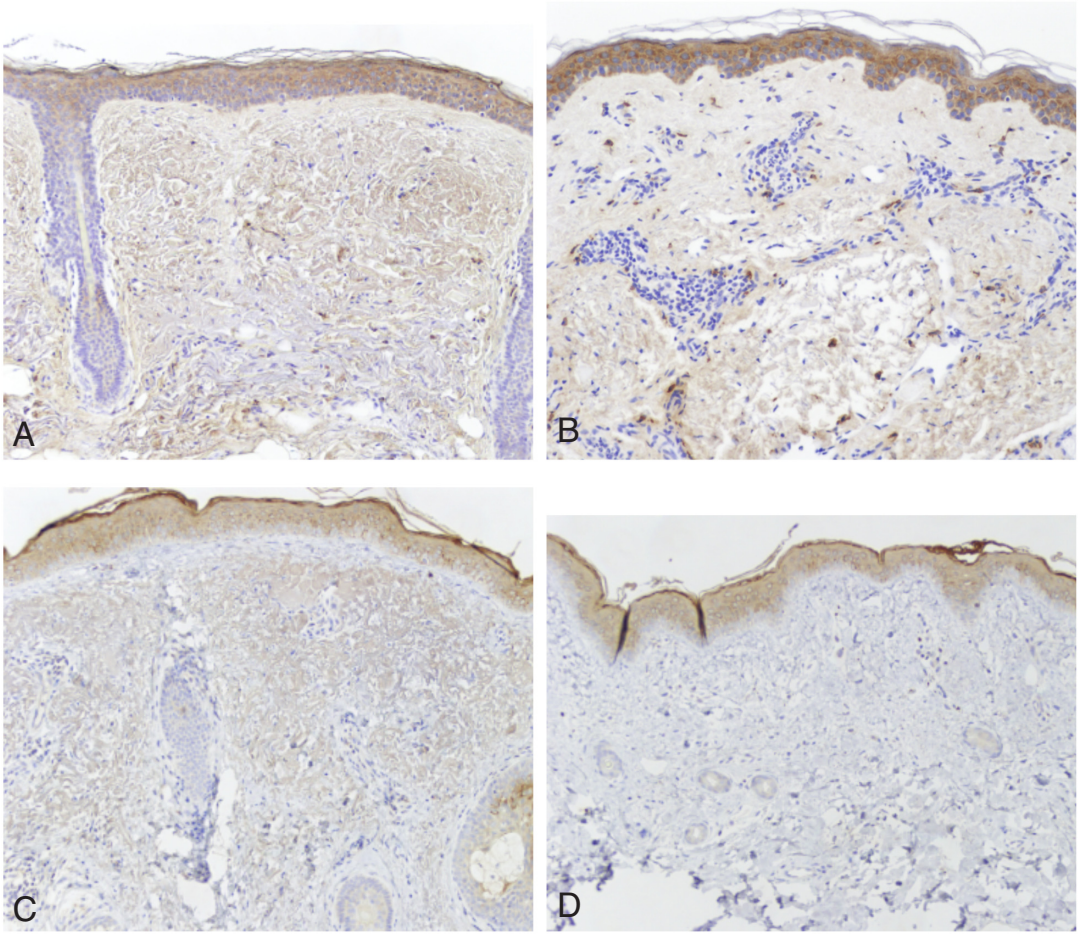

Fig. 5 Immunohistochemical staining for HO-1 and HO-2. Staining of HO-1 (A, B) and HO-2 (C, D). Representative sections of the ante-auricular skin (A, C) and post-auricular skin (B, D). (Original magnification x100).

HNE is a major and the most toxic aldehyde produced by the oxidation of ϖ-6 polyunsaturated fatty acids [5] and is considered the second toxic messenger of oxygen radicals [6]. HNE was increased in the ante-auricular skin (sunlight-exposed area) compared with the post-auricular skin (sunlig ht-protected area). Using double immunostaining, we further revealed that HNE was colocalized with degenerative elastin. In contrast, the content of 8-OHdG, one of the major oxidative base of DNA, was unchanged in the ante-auricular skin. These results suggest that chronic sunlight exposure predominantly induces the byproducts of lipid peroxidation. It has been reported that physiological concentrations of HNE exert growth-modulatory effects on cells via an epidermal growth factor receptor-linked signal pathway [15]. The treatment of macrophages or Kupffer cells isolated from cirrhotic liver with HNE has been found to consistently induce transforming growth factor β1 (TGF-β1) expression [16]. TGF-β1 is considered to be an essential growth factor in development, wound healing and fibrosis. This growth factor induces fibrosis and stimulates collagen and elastin expression [17]. These reports and our data suggest that HNE is involved at least to a certain extent in the elastotic changes in the ante-auricular skin. Chronic exposure to UV irradiation induced elastosis and degenerative alteration of skin structures. Nobuhiko T (Arch Dermatol Res 2001) reported that elastin, one of the extracellular matrix proteins, accumulated in HNE-positive areas in sunlight-damaged human skin [18]. Similarly, the colocalization of HNE and elastin was observed in the ante-auricular skin dermis (Fig. 3A). Interestingly, another extracellular matrix protein, collagen type I was not colocalized with HNE (Fig. 3B).

UVB also is a potent direct inducer of Mn-SOD activity in cultured human dermal fibroblasts, though with a delay of approximately 48 hours after UVB irradiation [19]. There are many reports on the roles of SOD, Cu/Zn-SOD and Mn-SOD in skin cells such as keratinocytes and dermal fibroblasts. Mn-SOD and Cu/Zn-SOD mRNA levels elevate immediately after UVA treatment [20]. Catalase expression also increases in human skin after high-dose UVB (4MED) irradiation [21–23]. However, in our study, Mn-SOD, Cu/Zn-SOD and catalase were observed in both the sunlight-protected epidermis and sunlight-exposed skins. These differences may be attributable to the exposure time (acute or chronic) with UV irradiation.

Heme oxygenase (HO), the rate-limiting enzyme in heme catabolism, catalyzes stereospecific degradation of heme to biliverdin, with concurrent release of iron and CO. In mammals, biliverdin is then converted to bilirubin by the cytosolic enzyme biliverdin reductase [10]. A previous study showed that induction of HO-1 in skin fibroblasts is of value in protecting against UV-induced oxidative stress [24]. Human skin fibroblasts

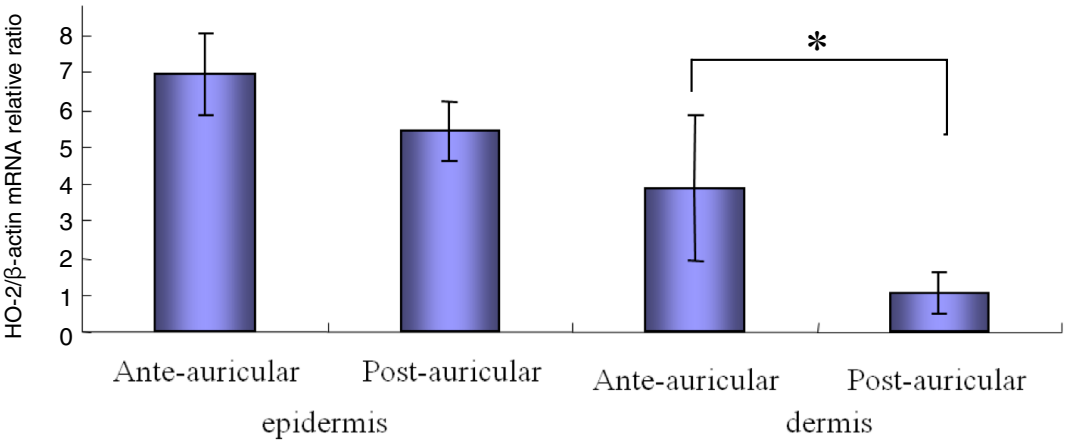

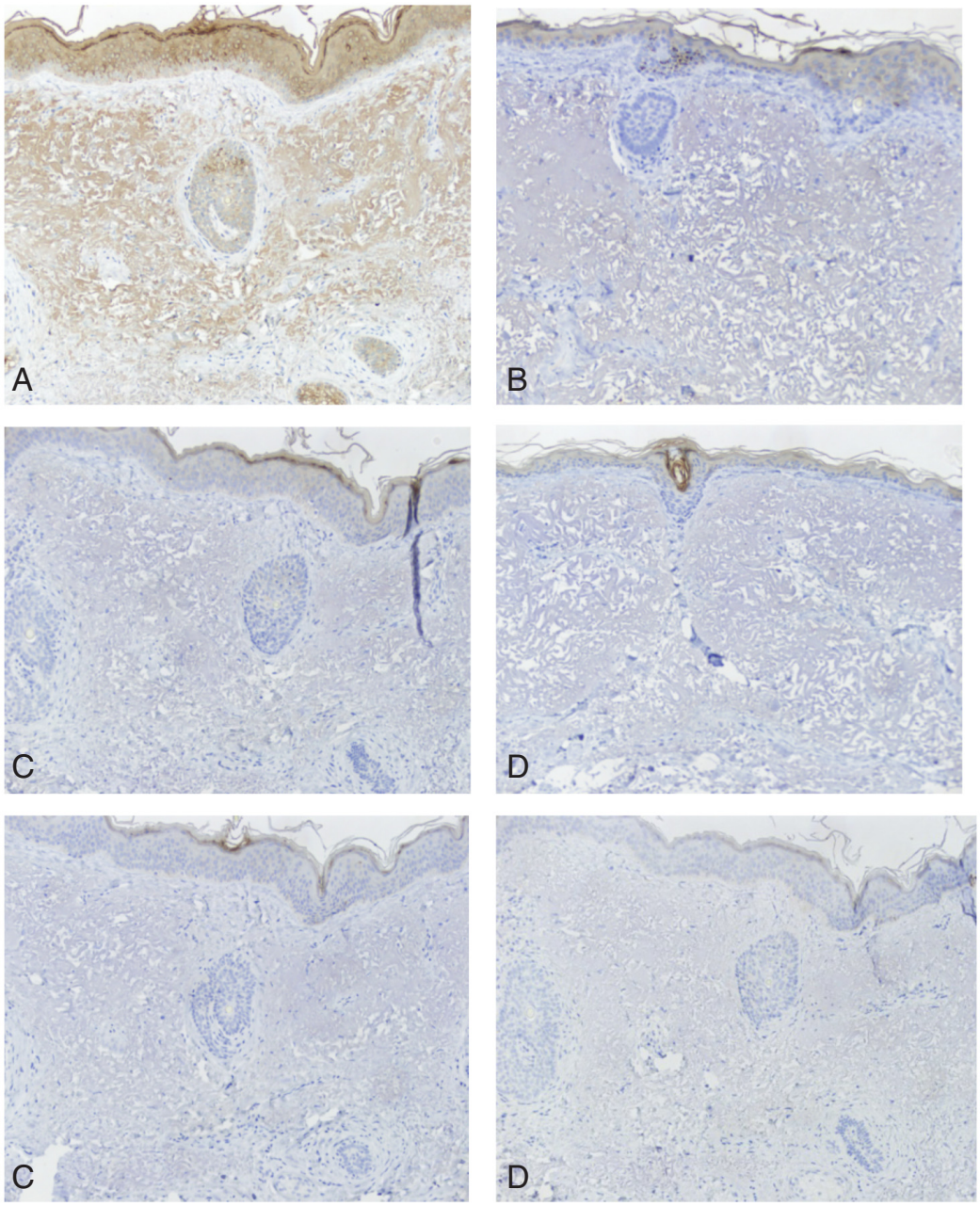

Fig. 6 Real-time RT-PCR analysis of HO-2 mRNA in the ante-auricular and post-auricular skins using laser microdissection, and absorption test for the specificity of anti-HO-2 antibody. (A) HO-2 mRNA expression was analyzed by quantitative real-time RT-PCR. *$p < 0.05$, $N = 5$. (B) Absorption test. One-milliliter aliquots of anti-HO-2 antibody solution (0.6 μg/ml) were reacted with synthetic HO-2 peptide at a concentration of (A) 0 μg/ml, (B) 0.006 μg/ml, (C) 0.066 μg/ml, (D) 0.6 μg/ml, (E) 6.6 μg/ml, or (F) 66.66 μg/ml. (Original magnification x100).

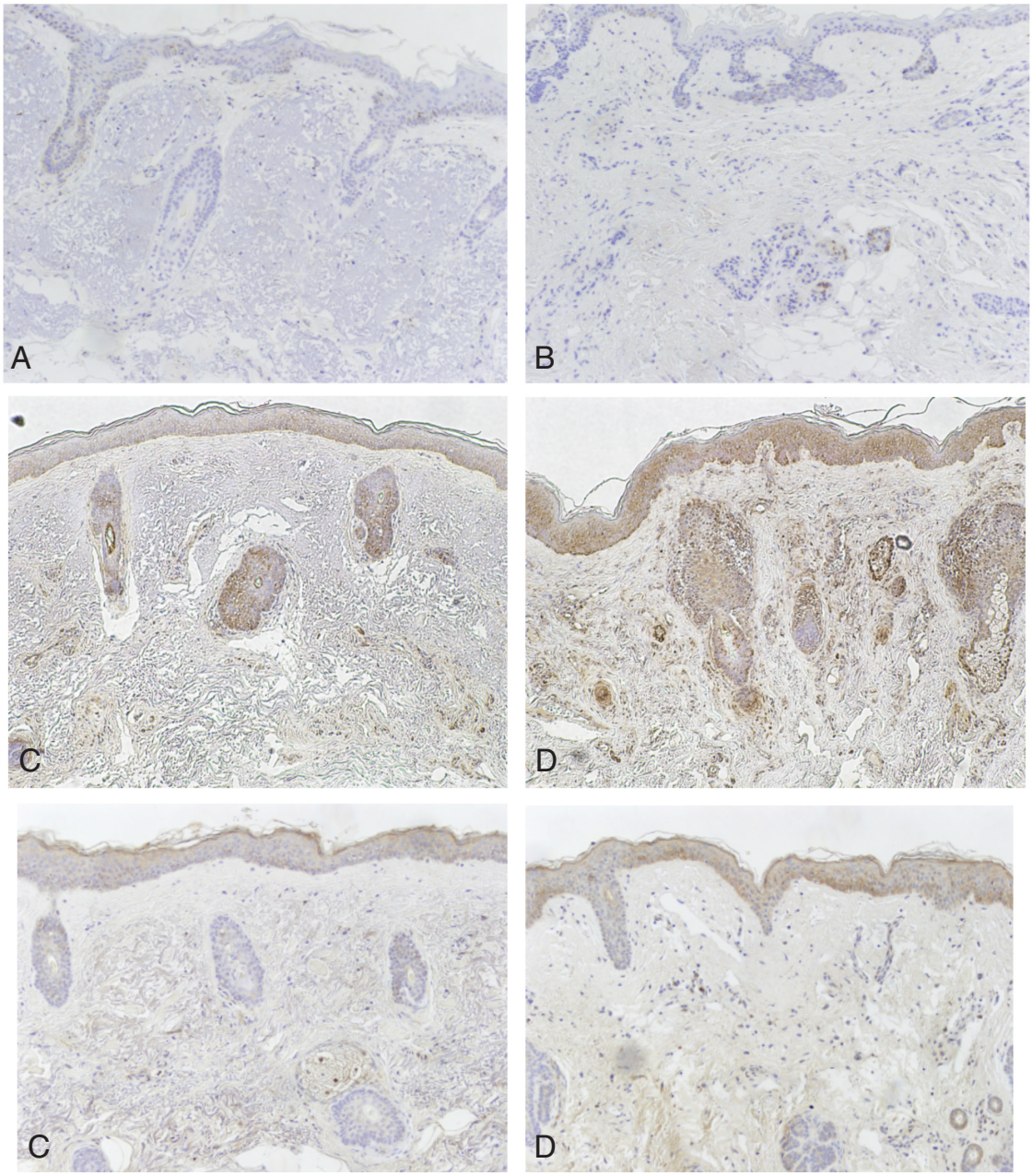

Fig. 7 Immunohistochemical staining for Mn-SOD, Cu/Zn-SOD and catalase in the ante-auricular and post-auricular skins. Staining of Mn-SOD (A, B), Cu/Zn-SOD (C, D) and catalase (E, F). Representative sections of the ante-auricular skin (A, C, E) and post-auricular skin (B, D, F). (Original magnification x100).

in culture respond to UV irradiation by increasing the expression of HO-1 [11]. Our data showed that HO-1 was expressed in the epidermis both in the sun-protected and sun-exposed skins with no significant difference. Furthermore, in the dermis, HO-1 was little or not at all expressed in several samples, macrophages or other inflammatory cells, but no detectable difference was observed in almost all samples. These findings demonstrate that HO-1 is not induced by chronic sunlight exposure.

HO-2 is unaffected by light stress and is moderately expressed in normal rat retina compared with the brain and testes that have the highest levels of HO-2 expression [25]. It has been reported that HO-2 mRNA levels are low in human dermal fibroblasts but high in epidermal keratinocyte. The role of HO-2 in the cell is not as well understood; however, it is becoming apparent that HO-2 may have an important role in epidermal cells [26]. HO-2 functions as a sensor of acute reduction in environmental O_2 by suppressing both native and recombinant Ca^{2+}-sensitive potassium channel activity, primarily through the production of CO [27]. And another inducer of HO-2 is CO and NO [28–30]. Furthermore, HO-2 is activated by calcium-calmodulin [31]. The phenomenon of UV-induced Ca^{2+} spectrum is a single peak at about 230 nm, UVB and UVA regions locating [32]. We showed that HO-2 was expressed in the epidermis of both the sun-protected and sun-exposed skins. In contrast, the expression of HO-2 was significantly increased in the sun-exposed

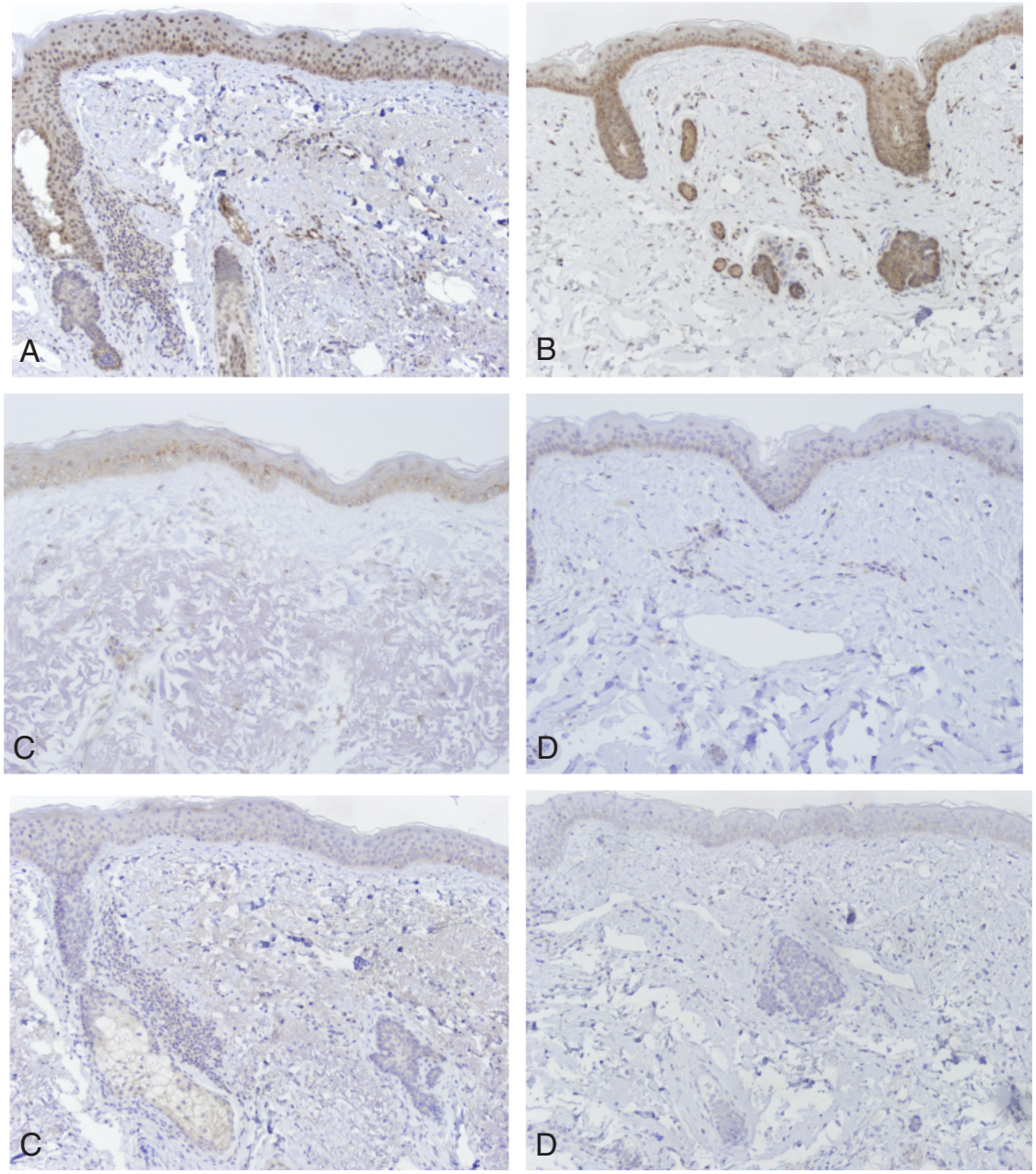

Fig. 8 Immunohistochemical staining for phosphorylated-p38 MAPK (phospho-p38), phosphorylated-JNK (phospho-JNK) and phosphorylated ERK (phospho-ERK) in the ante-auricular and post-auricular skins. Staining of phospho-p38 (A, B), phospho-JNK (C, D), and phospho-ERK (E, F). Representative sections of the ante-auricular skin (A, C, E) and post-auricular skin (B, D, F). (Original magnification x100).

dermis. Therefore, these observations suggest that HO-2 is induced by chronic UV-irradiation, but not by acute UV-irradiation. p38 MAPK, a signaling molecule, was activated in the sunlight exposed dermis. Activation of p38 MAPK may be related with the induction of HO-2. The detailed mechanism of HO-2 induction by chronic sunlight exposure remains to be determined.

Oxidative stress is implicated in the activation of signal transduction pathways and has been shown to induce phosphorylation of cell surface receptors, which in turn activates the MAPK signaling pathway [33]. The MAPK signaling molecules (p38 MAPK, JNK and ERK) are also activated by UV-induced oxidative stress. In our study, to examine the effect of chronic sunlight exposure on p38 MAPK, JNK and ERK, immunohistochemical study was performed using phospho-specific antibodies. We found that phosphorylation of p38 MAPK, JNK and ERK was most prominent in the ante-auricular epidermis, that of p38 MAPK and JNK in the post-auricular skins was more remarkable in the epidermis than in the dermis, and ERK was not phosphorylated at all in the dermis of both the ante- and post-auricular skins. In particular, phosphorylated p38 MAPK in the epidermis was increased in both the ante- and post-auricular skins, but that in the dermis was increased only in the ante-auricular skins, indicating a relationship between chronic sunlight-exposure and the depth of UV penetration. Chouinard *et al.* have shown that there was immediate activation

and a higher degree of JNK activity following UVA-irradiation (30 kJ/m^2) compared to UVB-irradiation (0.3 kJ/m^2) in human keratinocytes [34]. Low-dose UVB-irradiation (0.15 kJ/m^2) of human keratinocytes, caused immediate and prolonged phosphorylation of p38 MAPK that persisted for 48 h before returning back to basal levels [35]. UV irradiation strongly activates JNK and p38 MAPK, whereas ERK1/2 is only very weakly activated by comparison [37]. The JNK and the p38 MAPK pathways play differential roles in apoptosis triggered by UV [38]. These data, although from acute responses of human cell lines to UV-irradiation, point out the possibility that UV-induced activation of p38 MAPK and JNK is perpetuated upon chronic exposure to sunlight. Notably, one previous study has shown that UVA-induced p38 MAPK activity elicits Bcl-XL expression, which in turn provides protection against apoptosis [40]. Thus, it is possible that phosphorylated p38 MAPK appearing in the anteauricular epidermis and dermis as well as in the postauricular dermis prevents cell apoptosis in these layers of the skin Further investigation is warranted.

In summary, we demonstrated that chronic sunlight exposure induces degeneration of elastin in association HNE accumulation and HO-2 expression in the dermis. p38 MAPK may act as an important factor in oxidative stress-induced antioxidative responses and activation of signaling pathways. The detailed mechanism for the sequence of events following chronic sunlight exposure remains for further investigation.

ACKNOWLEDGMENTS

The authors thank Hideaki Hasegawa and Johbu Itoh at the Teaching and Research Support Center, Tokai University School of Medicine, for their technical support. This work was supported by a grant from the Tokai University School of Medicine Research Aid 2008 and 2009 and Grants-in-Aid for Scientific Research C (#21591446) from the Japan Society for the Promotion of Science, Japan.

REFERENCES

1) Harman D. Free radical theory of aging: an update: increasing the functional life span. Ann N Y Acad Sci 2006; 1067: 10–21.
2) Kasai H, Nishimura S. Hydroxylation of deoxyguanosine at the C-8 position by ascorbic acid and other reducing agents. Nucleic Acids Res 1984; 12: 2137–45.
3) Ahmed NU, Ueda M, Nikaido O *et al*. High levels of 8-hydroxy-2'-deoxyguanosine appear in normal human epidermis after a single dose of ultraviolet radiation. Br J Dermatol 1999; 140: 226–31.
4) Nishigori C, Wang S, Miyakoshi J *et al*. Mutations in ras genes in cells cultured from mouse skin tumors induced by ultraviolet irradiation. Proc Natl Acad Sci U S A 1994; 91: 7189–93.
5) Esterbauer H, Schaur RJ, Zollner H. Chemistry and biochemistry of 4-hydroxynonenal, malonaldehyde and related aldehydes. Free Radic Biol Med 1991; 11: 81–128.
6) Carini M, Aldini G, Facino RM. Mass spectrometry for detection of 4-hydroxy-trans-2-nonenal (HNE) adducts with peptides and proteins. Mass Spectrom Rev 2004; 23: 281–305.
7) Tanaka N, Tajima S, Ishibashi A *et al*. Immunohistochemical detection of lipid peroxidation products, protein-bound acrolein and 4-hydroxynonenal protein adducts, in actinic elastosis of photodamaged skin. Arch Dermatol Res 2001; 293: 363–7.
8) Darr D, Fridovich I. Free radicals in cutaneous biology. J Invest Dermatol 1994; 102: 671–5.
9) Maines MD, Panahian N. The heme oxygenase system and cellular defense mechanisms. Do HO-1 and HO-2 have different functions? Adv Exp Med Biol 2001; 502: 249–72.
10) Abraham NG, Kappas A. Pharmacological and clinical aspects of heme oxygenase. Pharmacol Rev 2008; 60: 79–127.
11) Keyse SM, Tyrrell RM. Heme oxygenase is the major 32-kDa stress protein induced in human skin fibroblasts by UVA radiation, hydrogen peroxide, and sodium arsenite. Proc Natl Acad Sci U S A 1989; 86: 99–103.
12) Lewis TS, Shapiro PS, Ahn NG. Signal transduction through MAP kinase cascades. Advances in Cancer Research, Vol 74 1998; 74: 49–139.
13) Aikawa R, Komuro I, Yamazaki T *et al*. Oxidative stress activates extracellular signal-regulated kinases through Src and ras in cultured cardiac myocytes of neonatal rats. Journal of Clinical Investigation 1997; 100: 1813–21.
14) Derijard B, Raingeaud J, Barrett T *et al*. Independent Human Map Kinase Signal-Transduction Pathways Defined by Mek and Mkk Isoforms. Science 1995; 267: 682–5.
15) Liu W, Akhand AA, Kato M, Yokoyama I, Miyata T, Kurokawa K, *et al*. 4-hidroxynonenal triggers an epidermal growth factor receptor-linked signal pathway for growth inhibition. J Cell Sci 1999; 112(14): 2409–17.
16) Leonarduzzi G, Scavazza A, Biasi F, Chiarpotto E, Camandola S, Vogel S, *et al*. The lipid peroxidation end product 4-hydroxy-2, 3-nonenal up-regulates transforming growth factor beta 1 expression in the macrophage lineage: a link between oxidative injury and fibrosclerosis. FASEB J 1997; 11(11): 851–7.
17) Roberts AB, Sporn MB, Assoian RK, Smith JM, Roche NS, Wakefield LM, *et al*. Transforming growth factor type beta: rapid induction of fibrosis and angiogenesis in vivo and stimulation of collagen formation in vitro. Proc Natl Acad Sci 1986; 83(12): 4167–71.
18) Tanaka N, Tajima S, Ishibashi A, Uchida K, Shigematsu T. Immunohistochemical detection of lipid peroxidation products, protein-bound acrelein and 4-hydroxynonenal ptotein adducts, in actinic elastosis of photodamaged skin. Arc Dermatol Res 2001; 293(7): 363–7.
19) Leccia MT, Yaar M, Allen N *et al*. Solar simulated irradiation modulates gene expression and activity of antioxidant enzymes in cultured human dermal fibroblasts. Exp Dermatol 2001; 10: 272–9.
20) Choung BY, Byun SJ, Suh JG *et al*. Extracellular superoxide dismutase tissue distribution and the patterns of superoxide dismutase mRNA expression following ultraviolet irradiation on mouse skin. Exp Dermatol 2004; 13: 691–9.
21) Muramatsu S, Suga Y, Mizuno Y *et al*. Differentiation-specific localization of catalase and hydrogen peroxide, and their alterations in rat skin exposed to ultraviolet B rays. J Dermatol Sci 2005; 37: 151–8.
22) Vayalil PK, Elmets CA, Katiyar SK. Treatment of green tea polyphenols in hydrophilic cream prevents UVB-induced oxidation of lipids and proteins, depletion of antioxidant enzymes and phosphorylation of MAPK proteins in SKH-1 hairless mouse skin. Carcinogenesis 2003; 24: 927–36.
23) Katiyar SK, Afaq F, Perez A *et al*. Green tea polyphenol (-)-epigallocatechin-3-gallate treatment of human skin inhibits ultraviolet radiation-induced oxidative stress. Carcinogenesis 2001; 22: 287–94.
24) Vile GF, Tyrrell RM. Oxidative stress resulting from ultraviolet A irradiation of human skin fibroblasts leads to a heme oxygenase-dependent increase in ferritin. J Bio Chem 1993; 268: 14678–81.
25) Kutty RK, Kutty G, Wiggert B *et al*. Induction of heme oxygenase 1 in the retina by intense visible light: suppression by the antioxidant dimethylthiourea. Proc Natl Acad Sci U S A 1995; 92: 1177–81.
26) Applegate LA, Noel A, Vile G *et al*. Two genes contribute to different extents to the heme oxygenase enzyme activity measured in cultured human skin fibroblasts and keratinocytes: implications for protection against oxidant stress. Photochem Photobiol 1995; 61: 285–91.
27) Williams SE, Wootton P, Mason HS *et al*. Hemoxygenase-2 is an oxygen sensor for a calcium-sensitive potassium channel. Science 2004; 306: 2093–7.
28) Ding Y, McCoubrey WK, Jr., Maines MD. Interaction of heme oxygenase-2 with nitric oxide donors. Is the oxygenase an intra-

cellular 'sink' for NO? Eur J Biochem 1999; 264: 854–61.
29) Adachi T, Ishikawa K, Hida W *et al*. Hypoxemia and blunted hypoxic ventilatory responses in mice lacking heme oxygenase-2. Biochem Biophys Res Commun 2004; 320: 514–22.
30) Shrestha Dangol D, Chen HP. Role of hemeoxygenase-2 in pregnancy-induced hypertension. Int J Gynaecol Obstet 2004; 85: 44–6.
31) Boehning D, Sedaghat L, Sedlak TW *et al*. Heme oxygenase-2 is activated by calcium-calmodulin. J Biol Chem 2004; 279: 30927–30.
32) Nakagaki T, Oda J, Koizumi H *et al*. Ultraviolet action spectrum for intracellular free Ca2+ increase in human epidermal keratinocytes. Cell Struct Funct 1990; 15: 175–9.
33) Assefa Z, Garmyn M, Bouillon R, Merlevede W, Vandenheede JR, Agostinis P. Differential stimulation of ERK and JNK activities by ultraviolet B irradiation and epidermal growth factor in human kerationocytes. J Invest Dermatol 1997; 108(6): 886–91.
34) Chouinard N, Valerie K, Rouabhia M, Huot J. UVB-mediated activation of p38 mitogen-activated protein kinase enhances resistanace of normal human keratinocytes to apotosis by stabilizing cytoplasmic p53. Biochem J 2002; 365(1): 133–45.
35) Pfundt R, Van VWI, Bergers M, Wingens M, Cloin W, Schalkwijk J. In situ demonstration of phosphorylated c-jun and p38 MAP kinase in epidermal keratinocytes following ultraviolet B irradiation of human skin. J Pathol 2001; 193(2): 248–55.
36) Hale KK, Trollinger D, Rihanek M, Manthey CL. Differential expression and activation of p38 mitogen-activated protein kinase alpha, beta, gamma, and delta in inflammatory cell lineages. J Immunol 1999; 162: 4246–4252.
37) Pavel Kovarik1, Monika Mangold, Katrin Ramsauer, Hamid Heidari, Ralf Steinborn2, Angelika Zotter, David E. Levy3, Mathias MuÈ ller2 and Thomas Decker. Specificity of signaling by STAT1 depends on SH2 and C-terminal domains that regulate Ser727 phosphorylation, differentially affecting specific target gene expression. The EMBO Journal 2001; 20 (1 & 2): 91–100.
38) Kohji Noguchi, Hironobu Yamana, Chifumi Kitanaka, Toshihiro Mochizuki, Akiko Kokubu and Yoshiyuki Kuchino. Differential Role of the JNK and p38 MAPK Pathway in c-Myc- and s-Myc-Mediated Apoptosis. Biochemical and Biophysical Research Communications 2000; 267 (1): 221–227.
39) New L, Han J. The p38 MAP kinase pathway and its biological function**.** Trends Cardiovasc Med 1998; 8: 220–228.
40) Michael A. Bachelor and G. Timothy Bowden. Ultraviolet A-induced Modulation of Bcl-XL by p38 MAPK in Human Keratinocytes POST-TRANSCRIPTIONAL REGULATION THROUGH THE 3_-UNTRANSLATED REGION. JBC 2004; 279 (41): 42658–42668.